Heliyon 10 (2024) e26941

Contents lists available at ScienceDirect

Heliyon

journal homepage: www.cell.com/heliyon

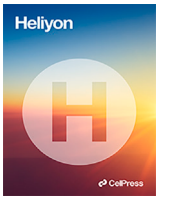

Research article

Robust tracking control of a minimal realization model of an impaired human hand for anthropomorphic coordination

Maryam Iqbal *, Junaid Imtiaz, Asif Mahmood

Department of Electrical Engineering, Bahria University, H-11, Islamabad, 47000, Pakistan

A R T I C L E I N F O

Keywords:
Hand biomechanical model
Central nervous system
Minimal realization
Tracking control

A B S T R A C T

Objective Physiologically relevant optimal controllers better represent the decision-making process of the central nervous system (CNS) with proper neural inputs and proprioceptor feedback. A biomechanical mathematical framework in the human palm reference frame was simulated using physiological dynamics to explore the biomechanics of movement coordination of fingers in a human hand.

Method Physiological state space models include multiple zero eigenvalues, representing a redundant system. A fingertip trajectory tracking control paradigm is created by reducing the model order through the H_∞ control paradigm. The external disturbances and sensory noise are included in the 21-Degrees-of-Freedom biomechanical model.

Main Results An analysis is conducted on the flexion movement of the robotic finger when it is disrupted from its initial equilibrium position. The controller administers feedback force at the joints to control the movement of the robotic finger. A full order H_∞ robust controller was developed, and the results were compared with the reduced-order model. The model order was reduced from 21 to 18 states. A reference trajectory is followed by the index finger in the minimal realization model, which is derived from the joint angular position profile. It stabilizes at a flexion angle of 1 rad/sec within 2 sec. Studying the simpler form of a model first gives a realistic view of the more complex model. This study has the potential to enhance our comprehension of anthropomorphic movement coordination in hands with impairments in kinesiology, ergonomics, assistive technology, and prosthetic devices.

1. Introduction

The hand is a structure of articulated, rigid components driven together by tendons with muscle actuation regulated by the central nervous system (CNS). The human hand possesses at least 20 degrees of freedom (DoF) due to the intricate mechanical interplay between the tendons, ligaments, muscles, and bones. Designing control techniques for a hand simulation model to regulate the fingertip's trajectory is challenging. By modeling the brain's processing of sensory input, a controller architecture that imitates the activities of the CNS seeks to address the complex challenge of movement coordination in numerous DoF. This way, a hierarchy of control mechanisms may be employed to replicate hand control [1]. On the most fundamental level, one can explain the kinematics and dynamics of each finger, whilst on the most advanced level, one must consider the movement coordination and position control of the fingers that comprise a hand. Lower-level control of the human hand involves neuromuscular control of the finger position.

* Corresponding author.
E-mail address: maryamiqbal.buic@bahria.edu.pk (M. Iqbal).

https://doi.org/10.1016/j.heliyon.2024.e26941
Received 24 March 2023; Received in revised form 20 February 2024; Accepted 21 February 2024

Available online 27 February 2024

This control is required to support the higher level grasp style control frequently emphasized in robotics and prosthetics. Loss of a hand or its functions, whether acquired or congenitally present, is a life-changing occurrence that creates significant obstacles in rejoining a regular lifestyle. It can impede the ability of a person to perform ADLs and significantly reduce their standard of living. The critical role that a hand plays in our ability to interact with our surroundings is painfully evident when one loses a hand or the functionality of a hand. The ability to maintain movement coordination between the digits of a human hand is a crucial skill regulated by the CNS, which contributes to the practical functionality of a human hand. The decreased cost of testing hypotheses, prosthetic models based on visco-elastic parameters, and surgical repair procedures strongly motivate developing, simulating, and controlling an anatomically precise model for the human hand.

It is a prevailing occurrence for the human hand to exhibit partial impairment rather than complete loss of function. A partial disability would manifest as the loss of a thumb and a few fingers while the remaining digits continue to function normally. The loss of motor skills experienced by this subset of amputees can profoundly affect their daily lives and their ability to continue working at the same capacity. Out of these, 73% of the partial hand amputees have returned to work, but 66% had to look for new employment because of the amputation [2].

Revolutionary prosthetics for a partly disabled human hand are considered essential. The fundamental challenge in developing a prosthetic or wearable device for individuals with partial disabilities lies in effectively coordinating the CNS with anthropomorphic fingers. Prosthetic devices for patients with partial hand amputations have come a long way in recent years [3,4].

In their study, as detailed in [5], the researchers explore an innovative application of sliding mode control, termed Biomimetic Sliding Mode (BSM) control, contrasting it with a proportional-derivative (PD) force controller. The BSM controller is engineered to interpret signals from human muscles into directives for the prosthetic motor, replicating physiological predictability. Results indicate that the BSM controller closely mirrors the control mechanisms observed in the human hand regarding position and force.

Within the realm of anthropomorphic robotic and prosthetic hand development, Kontoudis et al. [6] discuss a compliant finger design that is underactuated, capable of flexion/extension and adduction/abduction movements, enabling robust grasping and dexterous manipulation without slippage.

Furthermore, Chen et al. [7] propose a hybrid control strategy for a five-fingered, 14-DoF robotic hand. This approach integrates soft control, utilizing an Adaptive Neuro-Fuzzy Inference System (ANFIS) and fuzzy logic (FL), with hard control employing proportional-derivative control (PD). Simulation outcomes reveal that the hybrid PD controller, calibrated with FL, surpasses the performance of either hard control or soft computing alone.

These studies shed light on the intricate yet promising avenues within robotic and prosthetic hand development, offering insights into novel control strategies that mimic physiological processes and enhance functionality in real-world applications. Such advancements hold immense potential for improving the quality of life for individuals with limb impairments, providing them with more natural and intuitive control over prosthetic devices.

In their research described in [8], developing a novel force myography (FMG) sensor marks a significant stride in prosthetic technology, particularly for individuals with trans-radial amputations. By utilizing FMG signals as control inputs instead of traditional electromyography (EMG), this approach offers a more cost-effective solution for hand prostheses. The study introduces two distinct control strategies—proportional control and a fuzzy logic-based classification system—tailored to operate specially designed prosthetic hands. Notably, the fuzzy logic (FL) classification approach showcased superior offline performance metrics, including accuracy, sensitivity, and precision, indicating its potential for real-world implementation.

Meanwhile, the field of biomedical engineering continues to witness advancements in the classification and prediction of finger movements, as demonstrated in [9]. The introduction of the Multi-centered Binary Pattern (MCBP) method presents a novel approach to classifying finger movements, showing promise with its 4% improvement in accuracy over existing methods. Such innovative techniques enhance our understanding of human motion and pave the way for more effective and intuitive control mechanisms in prosthetic devices.

These developments underscore the evolving landscape of prosthetic technology and biomedical engineering, where interdisciplinary research efforts converge to address the unique needs of individuals with limb impairments. By leveraging novel sensor technologies and advanced classification algorithms, researchers strive to create prosthetic solutions that offer improved functionality, affordability, and user experience, ultimately enhancing the quality of life for individuals with upper limb loss.

In the study by Luo et al. [10], a biomimetic controller integrates neuromuscular reflex features. The researchers demonstrate that this integration can lead to human-like force regulation, hence improving the motor performance of amputees utilizing a tendon-driven prosthetic hand. Nevertheless, the functionality of these devices is constrained due to the absence of sophisticated user control choices [11].

Designing a prosthetic device that incorporates anthropomorphic robotic fingers with the ability to replace a partially functional hand efficiently presents substantial challenges. The successful execution of this undertaking necessitates a comprehensive examination of the synchronization between the motions of robotic digits and human digits, with their incorporation into the CNS. The comprehensive design of the prosthetic hand incorporates several factors, such as human anatomy, mechanical mechanisms, sustainable power supply, and the restoration of functional abilities. Moreover, exploring the complex intricacies of human finger movements is crucial and requires comprehensive examination and improvement.

There is great potential for progress in CNS research in developing a computational model of the brain controller guided by physiological considerations to attain high precision. However, two main challenges make human finger modeling and control more difficult in prostheses. These problems stem from the intricate nature of the human hand's biomechanics and the complexities involved in replicating natural finger movements artificially.

Redundant manipulators refer to robotic systems with excess DoF beyond the minimum required to execute a specific primary task using an end-effector [12,13]. The human arm and hand are typical examples of redundant systems. In recent years, the concept of redundant robotic arms has garnered significant attention within the robotics community, owing to their ability to address complex challenges while simultaneously meeting supplementary requirements effectively. Various techniques for managing them have been the subject of extensive scholarly research, including monitoring joint and task spaces and optimizing performance criteria and null space. The authors investigated robot manipulator velocity-level and acceleration-level redundancy-resolution equivalence in [14]. Both schemes were reformulated as solvable quadratic programmes. Redundancy-resolution systems at distinct joint velocity and acceleration levels are equal, contributing to a significant and novel discovery. Wiedmeyer et al. [15] proposed a redundancy resolution strategy for seven-DoF serial manipulators. This approach was integrated into a fully analytic Inverse Kinematics (IK) solution, improving motion times along prescribed Cartesian paths. Redundancy is a valuable feature that offers adaptability and the ability to quickly recover from lost control and adjust to changing circumstances. Nevertheless, the computational challenge of effectively controlling multiple DoF remains a significant concern in cognitive robotics and anthropomorphic prosthetic hands, where achieving precise and intentional control is essential [16]. These concerns are addressed in [13,17,18]. The authors of the study in [19] aim to establish a correlation between the resolution of redundancy in robotic arms and the resolution of redundancy in the human arm during point-to-point reaching tasks.

Despite the human hand being an object with great articulation, it is also subject to a significant degree of constraint. This complexity is highlighted by the challenges that robotics and neuro-prosthetics face when controlling the most recent generation of anthropomorphic hands. There are inter-dependencies between the different joints of a finger and between the digits of a human hand. Such motion limitations implicitly specify the natural movements made by human hands [20]. The study of such constraints is vital for the proposed modeling and control scheme to be physiologically relevant to the natural hand.

Zanchettin et al. [21] found a direct correlation between hand position and self-motion angle within the framework of human arm movement. The aforementioned relationship was then modified to facilitate the replication of human-like motion by redundant anthropomorphic manipulators while also maintaining adherence to the overall orientation limitations for the hand. The utilization of the Saturation in Null Space (SNS) technique, as proposed by Flacco et al. [22], is implemented as a solution for addressing the complexities associated with inverse kinematics in redundant robot systems. The method exhibits versatility as it is adept at managing both single and multitask situations while also guaranteeing adherence to restrictions about joint angular locations, velocities, and accelerations. The critical positions and end-effector orientation constraints restrict the inverse kinematics, allowing an efficient analytical scheme to construct human-like configurations. Various methods have been suggested for the direct resolution of inverse kinematics while incorporating additional constraints [23–26].

As system links increase, formulating motion equations becomes more complex and time-consuming. However, a recursive formulation can automate the governing equation derivation, solving this problem. Recursive procedures are especially advantageous in the context of open kinematic chains. Utilizing a recursive methodology can streamline the intricate process of deducing motion equations. Recursive algorithms partition the system into smaller segments or components, enabling a sequential analysis. This methodology initiates from the foundational link and proceeds towards the terminal effector, methodically computing the kinematic and dynamic variables and the resultant forces exerted on every segment.

The authors introduce a revolutionary method for controlling the trajectory of a serial robotic manipulator represented as a dynamic model in their study described in [27]. An autonomous wheeled movable platform supports the manipulator's numerous linkages, which are joined by revolute joints. The methodology employs an iterative process to compute the dynamic and control equations of the system automatically, aiming to streamline computational complexity and determine optimal input control torques and velocities for the robotic system, even in the presence of uncertainties. This innovative methodology holds significant implications for robotics research and application. Automating the computation of dynamic equations and control strategies offers a more efficient and systematic approach to designing and optimizing the performance of robotic manipulators. Additionally, by addressing uncertainties in real-world operating environments, such as variations in terrain or external disturbances, the methodology enhances the robustness and reliability of trajectory tracking control, contributing to safer and more precise robotic operations.

A recursive approach (Runge-Kutta Method) and computer simulations are employed to validate the motion planner and control strategies of a novel adapted mobile linear robotic system with an n-link robotic arm on a mobile slider along a rail, as presented in [28]. Innovative centralized control algorithms for system navigation towards an unattainable objective are developed using the Lyapunov-based Control Scheme (LbCS). The technique helps the unanchored manipulator reach tasks. Similarly, for serial robots with a reasonably large number of joints, recursive algorithms that are computationally efficient are proposed in [29,30].

Developing strategies for generating human-like motion is currently a topic of research interest [31]. Kim et al. [32] proposed an algorithm for estimating swivel angle in a 7-DoF exoskeleton system that integrates kinematic and dynamic criteria. This algorithm aims to replicate the natural motion of the human arm. The issue at hand pertains to the challenge of ascertaining the respective weights of the two criteria. Liu et al. [33] introduce essential positions for anthropomorphic 7-DOF redundant manipulators, such as Cartesian elbow and wrist joint positions, for optimal redundancy resolution. This approach is only intended for the replication of motion in real-time.

In order to perform specific and repetitive tasks effectively, control algorithms commonly employed in robotics and prosthetics have typically focused on rigid multibody systems with a restricted range of DoF. The authors in [34] employed a proportional-integral (PI) position controller to facilitate functional grasping activities for individuals who have experienced a stroke, utilizing a power-assisted glove. The Harvard robotic glove utilized a sliding-mode controller that was model-free in order to effectively regulate the pressure exerted on the soft actuators [35]. Model-free procedures eliminate the need for a comprehensive dynamic model in such systems, distinguished by their significant compliance, enabling them to adjust to diverse conditions and deformations. Nevertheless,

the efficacy of these methodologies heavily relies on the consistency and dependability of the system in question. In simpler terminology, these model-free methods demonstrate effective performance when the system exhibits consistent and predictable behavior. However, when confronted with substantial changes or uncertainties in the behavior of the system, its effectiveness is reduced. This limits their application to repetitive operations with minimal environmental or system changes. Thus, they are unsuitable for tasks that require adaptability and robust performance in changing conditions or unanticipated problems. Jeong et al. introduced the concept of the Exo-Glove with soft tendons, which employs a position-based impedance control (also known as admittance control) mechanism, as outlined in their work [36]. This novel methodology enables the tendons to replicate the characteristics of a pliable spring, hence enhancing their capacity to adapt to a wide range of tasks. However, a notable constraint of this mechanism is its inability to offer personalized control for each joint, a crucial requirement for intricate motions.

Additionally, human motion can also be replicated with the use of impedance control [37] and differential kinematics [38]. This paper presents a methodology for generating a human-like joint angular position trajectory incorporating a unique perspective on tracking control of an anthropomorphic impaired human hand.

The primary objective of the research outlined in [39] is to assess the effectiveness of a high-order biomechanical bond graph model, specifically a model of 21^{st} order. This model is coupled with a physiologically inspired Linear Quadratic Regulator (LQR) to optimize costs associated with impaired hand functionality. The current study incorporates considerations of physiological costs involved with the monitoring of position control and voluntary motions of a robotic finger within a partially functional hand in the design of the controller. This comprehensive approach seeks to develop a controller that not only enhances control performance but also maximizes the energy efficiency of the system, aligning both objectives for an optimal outcome.

Our current research represents a natural progression of the previously proposed modeling and control framework in [40]. In this extended research phase, we introduce the LQG Integral (LQI) control method into the existing framework. The integration is achieved by utilizing the graphical method of bond graph modeling to create a detailed mathematical representation that accurately captures the movements of a human-impaired hand.

We have conducted a rigorous sensitivity analysis to assess the robustness of the model and its ability to faithfully simulate real-world scenarios characterized by disturbances. This analytical process entails examining how the model responds to parameter and input variations. This sensitivity analysis has demonstrated a remarkable convergence between sensitivity in the model and that in the physical system, underscoring the model's reliability and capacity to replicate real-world behavior faithfully.

One pivotal aspect of our investigation revolves around developing a robust and optimal compensator. This compensator is designed specifically to address the complexities of a 21^{st} order biomechanical model. By utilizing integral control techniques, our goal is to improve the system's performance, especially when dealing with uncertainties, disturbances, and noisy sensor inputs. Our research, therefore, contributes to advancing the field of biomechanical modeling and control by providing insights into the design of effective compensatory mechanisms for human-impaired hand systems.

The genesis of H_∞ control theory stemmed from the imperative to tackle multifaceted challenges in control system design. These challenges encompass dynamic uncertainties, external inputs, the pursuit of optimal performance criteria, and the incorporation of user-defined weighting functions during the controller synthesis process. The literature extensively records the thorough examination of these issues within the realm of H_∞ control theory, highlighting the theory's capacity to effectively manage these intricate aspects of control system design [41]. As outlined in [42], when dealing with a nominal model and employing a full order or unstructured controller, the classical sub-optimal H_∞ control problem can be reformulated as a convex problem. To enhance the precision of system modeling, it is essential to elevate the order of the nominal model, thus leading to a higher order of the controller. The constraint mentioned in this context hinders the actual use and implementation of unstructured H_∞ controller synthesis methods, as outlined in [43]. When dealing with reduced-order models of impaired human hands, achieving a harmonious equilibrium between computational efficiency and the requisite level of accuracy for the particular objectives at hand is imperative. It is essential to meticulously evaluate the benefits and drawbacks outlined above within the framework of the specific disabilities being simulated and the objectives of the examination or implementation.

Frequency domain control approaches such as PI, PD, and proportional-integral-derivative (PID) configurations are prominent in all control schemes due to the availability of extensive literature and standard methods. Stability analysis using proprioceptive input is one area of biomechanical modeling to which these controllers have significantly contributed. In [44], the authors proposed a fuzzy PID control technique for achieving the grasping force control and mitigating the impact of modeling error for an artificial human hand. The authors demonstrated through simulations and experiments that the proposed approach is reasonably practical in tracking the reference grasping force even when an external disturbance is present.

In the study by Raj et al. detailed in [45], the researchers introduced a control approach for a prosthetic hand. This method operates through surface electromyography (sEMG) input and employs a PID control scheme. Given its low cost and ease of operation, a geared DC motor was chosen for the actuating structure of this prosthetic hand, and the proposed method provides a good performance and control strategy. The primary issue with traditional control methods is that for higher-order MIMO systems, a separate controller needs to be constructed to regulate each state. This is a requirement that must be considered. In addition, biological systems develop nonlinear properties, and the PID controller fails to show promising results in most of the literature cited above due to oscillations and unfavorable deviation in angular profiles.

The dynamic controller designs developed earlier in [39,40] are for a 21^{st} order system that controls the linear plant model, which demands more computational efforts. Redundant states that do not significantly contribute to the dynamics of the system under consideration are sometimes included in high-order models. As a result, reducing the model order while maintaining model characteristics is always preferred. Several eigenvalues in the physiological models are zero, and the models are intrinsically redundant. The controller design that considers the information about the entire system is more complex but can be reduced to a lower order.

The CNS initiates the movement of every finger in a biomechanical system. The generation of intent starts the desired activity. The CNS can instantly sense the finger's exact position and assesses the required joint angles. The CNS sends specific commands to the relevant muscles through nerves, which then start the movement of the fingers. This explanation elucidates the anatomical structure and function of finger joints, highlighting the crucial role of tendons in enabling mobility. This comprehension is the basis for the future creation of an extensive biomechanical model.

This paper presents a unique approach to control an anthropomorphic index digit within a human hand with certain functional limits. The proposed methodology aims to achieve robustness and optimality by utilizing H_∞ control techniques. Our study presents a robust control synthesis framework that integrates the CNS into the mathematical representation of a biomechanical system. Despite sensor noise and small perturbations, the simulation results demonstrate that the proposed methodology maintains stability and robustness. The minimal realization method is implemented to achieve the pole-zero cancellation of the transfer function. This procedure also eliminates the uncontrollable and unobservable states from the proposed biomechanical state space model. A full order H_∞ robust controller is developed, and the results are compared with the reduced order model. The model order was reduced from 21 states to 18 states. The stable response of the full order plant shows that the three states eliminated due to minimal realization are stabilizable and detectable. This information can be beneficial in the practical application while designing a prosthetic hand in future. This study only coordinates one robotic digit with the rest of the normal digits and CNS.

Additionally, it is demonstrated that the proposed angular position tracking control method guarantees the uniform boundedness of all signals in the closed-loop system. Moreover, by appropriately selecting the design parameters, the position tracking errors can converge to a desirable value of negligible magnitude.

Assessing the extent to which the proposed model effectively handles the problem of trajectory tracking offers substantiation for the efficacy and significance of the approach. The estimation of actuation force in relation to the proximal interphalangeal (PIP) joint trajectory was achieved by including a feedback signal from the controller. Determining actuation force is of utmost importance as it enables the model to replicate the observed biological muscle function involved in coordinating finger movements. The aim of reproducing this mechanism in force actuation at the phalanges is to attain coordination and movement patterns that closely resemble the natural hand functions observed in humans while ensuring reliable tracking control.

By integrating the concept of estimating actuation force based on the PIP joint trajectory, the robust tracking control approach demonstrates a consideration of the underlying biomechanics of the hand. This contributes to a more realistic and natural robotic hand movement, enhancing coordination and dexterity in performing tasks. Overall, this research highlights the merit of the proposed H_∞ control method by showcasing its robust performance in trajectory tracking. The utilization of the feedback signal to estimate actuation force and mimic the biological muscle function in finger coordination brings our model closer to replicating the intricacies of natural human hand movements.

The paper begins by providing an overview of the conception and mathematical formulation of the biomechanical model, which serves as a foundational basis for the subsequent sections. Subsequently, the study conducts a thorough analysis of the model's stability, effectiveness, and precision in maintaining accuracy under various conditions and perturbations, offering crucial insights into its overall robustness and tracking control. Furthermore, this research comprehensively discusses simulation results, drawing meaningful comparisons with previous studies. These findings underscore the effectiveness of the proposed H_∞-synthesis-based control approach and contribute to the broader body of knowledge in neurophysiology and biomechanics.

2. Bond graph modeling technique

Mathematical models are employed extensively to gain insight into the structure and performance of biomechanical systems. The study of neuromuscular factors related to finger mobility in the human hand can benefit from these models. Students and researchers may be stymied in their attempts to gain fresh insights into the biomechanical systems due to the time and effort required to refine a model. Model optimization may be enhanced in several ways, using techniques derived from bond graph modeling [46,47]. The bond graph modeling technique offers a unified method for representing a system composed of two or more energy systems. Although bond graph approaches have been successfully implemented in many applications, their implementation in biomedical engineering has been relatively limited [48]. There is a need for a unified modeling approach in biomechanics, as it deals with multi-dimension systems. Mathematical models of mechanical and electrical systems interacting with and controlling musculoskeletal and neurological components may be essential for future advancements in assistive technology.

Once the model is graphically represented, general system equations are derived, solved numerically, and analyzed. The $n \times 1^{st}$ order equations are generated by simply interpreting the graph. It is helpful for various physical-system modeling, investigation, control, and fault-diagnosis tasks.

2.1. Multi-link bond graph model of the impaired hand

The initial step before delving into an intricate bond graph is to establish a fundamental model of a single phalanx and joint. A finger's kinematic chain connects three rigid bodies through movable joints. The proximal interphalangeal (PIP) joint is located nearest to the palm, while the distal interphalangeal (DIP) joint is situated at the far end. Tendons are crucial for linking muscles to bones and facilitating movement in joints. The palm also connects with the metacarpophalangeal (MCP) joint. The holistic biomechanical model examines the DIP, PIP, and MCP joints in all four fingers.

Eq. (1) presents the natural intra-finger constraints on the angular displacement of the PIP and DIP joints in the human hand, as documented in various research works [49–51]. As mentioned earlier, the constraint is significant in our research work, as it is

Table 1
Static constraints on index & middle finger.

Index/Middle Finger	Maximum Flexion Angle	Maximum Extension Angle
θ_{PIP}	100°	0°
θ_{DIP}	80–90°	5°

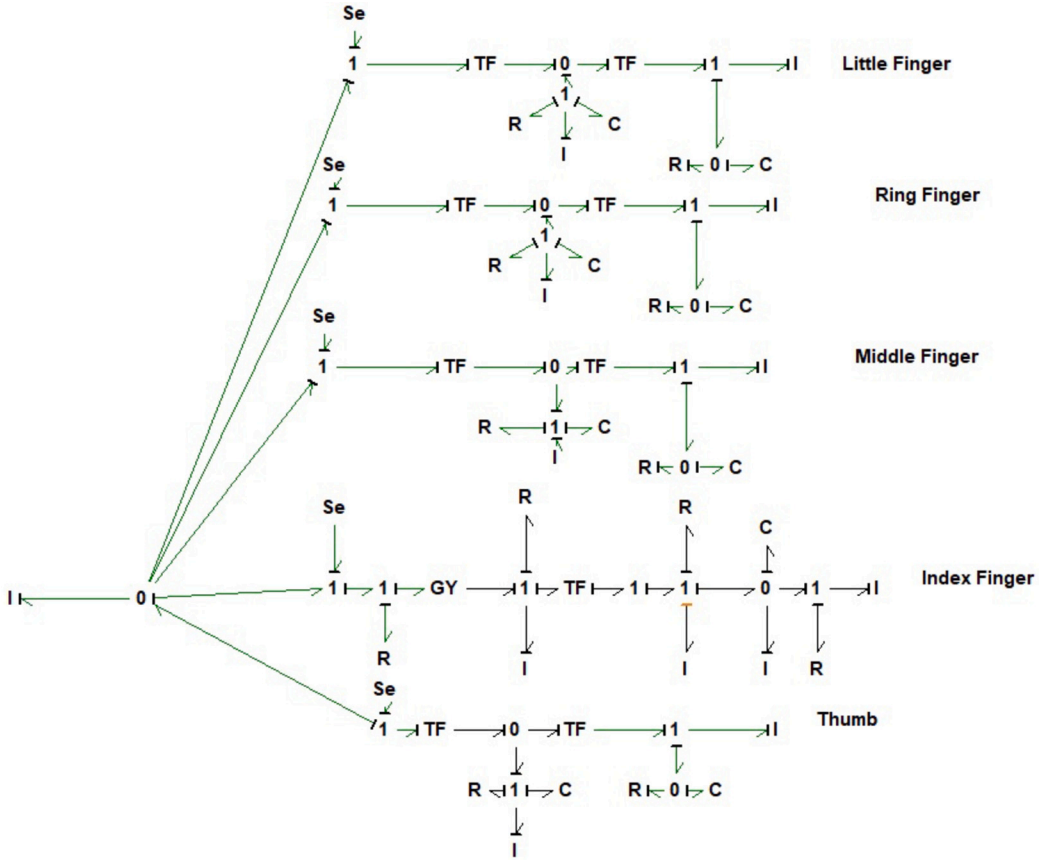

Fig. 1. Illustration of the model's dynamics in a bond graph.

incorporated into our proposed framework to reduce the redundancy of the model. This constraint is integrated into the bond graph model as the modulus of the transformer ratio between PIP and DIP joints.

The static constraint refers to the limits of the range of finger motions due to the hand anatomy. The constraints are given in Table 1.

One of the predominant notions, based on the anatomical structure of the hand, is that in order to flex the DIP joints of the index, middle, ring, and little fingers, a simultaneous flexion of the corresponding PIP joints is necessary. The mathematical representation of the intra-finger constraint is integrated into the biomechanical model being suggested, as outlined in Eq. (1):

$$\theta_{DIP} = \frac{2}{3}\theta_{PIP} \tag{1}$$

The study described in [40] presented a bond graph model that was developed to represent the complex biomechanics of a human hand. This model included both the natural fingers and a prosthetic anthropomorphic finger, which was created to replace an impaired index finger. This model can effectively handle biomechanical redundancy by combining the PIP and DIP joints. A vital element of this approach is representing the wrist joint as an inertial mass, denoted as 'I,' and simulating it using a combination of two hinge joints. The design of the index finger model is inspired by the advanced lead screw mechanism used in modern bionic hand technology, as explained in the study conducted by Slade et al. [52]. By including this, the model becomes more accurate and highlights its relevance and applicability to the latest breakthroughs in the sector. The intricately designed model's dynamics are illustrated by a thorough bond graph, visually depicted in Fig. 1, which provides a comprehensive understanding of the interconnected components and their interactions. The details of the elements and the bond graph terminologies are given in Appendix A.

Eq. (2) and Eq. (3) provide the generic state-space equations that form the basis of the 21^{st} order model constructed by the proposed modeling technique.

$$\dot{\vec{x}}(t) = A\vec{x}(t) + B\vec{u}(t) \tag{2}$$

$$\vec{y}(t) = C\vec{x}(t) \tag{3}$$

In this context, $\vec{x}(t)$ denotes the states of the biomechanical model that hold physiological relevance, encapsulating various dynamic aspects of the system at time t. The vector $\vec{u}(t)$ represents the input control provided by the compensator, mimicking the actions orchestrated by the CNS to regulate and influence the behavior of the system. Lastly, $\vec{y}(t)$ signifies the output measurement accessible for feedback.

Here, $A \in R^{21\times21}$ represents a state matrix, giving the dynamics of the 21 states of the partially impaired human hand. $B \in R^{21\times1}$ is the input matrix. C represents an output matrix such that $C \in R^{1\times21}$.

The model has five input sources (Se1–Se5). These sources depict natural human-hand MP joint forces. As seen in Fig. 1, the 2-port transformers and 3-port 0-junction and 1-junction components effectively depict torque distribution across joints. Using the simulation system depicted in Fig. 1, it is observed that applying a voltage of **V** to the motor at the MCP of the mechanical finger causes it to rotate, resulting in an angular displacement $\vec{\theta}(t)$.

There are 12 inertia elements and nine stiffness elements, giving 21 elements that store energy. The variables **p** and **q** reflect each inertial element's generalized momentum and displacement. Eq. (4) gives the state vector $\vec{x}(t)$.

$$\vec{x}(t) = [p_1\ p_2\ p_3\ q_1\ p_4\ p_5\ q_2\ q_3\ p_6\ q_4\ q_5\ p_7\ p_8\ q_6\ q_7\ p_9\ p_{10}\ q_8\ q_9\ p_{11}\ p_{12}\ ]^T \tag{4}$$

When power is supplied to the motor of the robotic finger, it initiates a series of dynamic responses within the system. This process is characterized by the transfer of energy through the motor, resulting in mechanical motion observed at the intermediate and distal phalanges of the index finger. These phalanges possess a cumulative inertia that influences the overall behavior of the system.

To quantify this behavior, we introduce the state variable $\vec{x}_3(t)$, which encapsulates the total angular momentum of the intermediate and distal phalanges, represented as $\vec{p}_3(t)$. The angular velocity of the finger's motion denoted as $\vec{\omega}(t)$, is computed by dividing the total momentum by the rotational inertia, symbolized as I. This calculation provides insight into the rate of change of angular displacement, indicating how quickly the finger is rotating.

By integrating the vector function $\vec{\omega}(t)$, we derive the output corresponding to angular displacement, represented by the vector $\vec{\theta}(t)$. This angular displacement captures the actual movement of the finger and serves as a crucial metric for assessing the effectiveness and accuracy of the control system. Overall, this process illustrates the dynamic interplay between power input, angular momentum, and angular displacement in governing the motion of the robotic finger.

3. Control synthesis of an impaired human hand

The integrated kinematic system model, coupled with proprioceptive feedback, presents an avenue for deeper exploration by applying controller strategies, enriching our understanding of physiological systems. By incorporating physiological constraints, we can assess the importance of these feedback control dynamics in governing hand movements. In addition, the proposed model would include feedback delays to facilitate simulation-based studies on the coordination between human hand digits and the CNS. This approach allows us to examine the impact of feedback systems on the dynamics of hand movements, offering vital insights into the complex interaction between sensory inputs and motor responses. By implementing feedback delays in the model, we can investigate the influence of various temporal aspects on the coordination and synchronization of movements, providing insight into the fundamental principles of motor control. In summary, this comprehensive approach holds the potential to improve our comprehension of the physiological foundation of hand movements and guide the creation of more efficient control methods for robotic and prosthetic systems.

4. Compensator design

4.1. H_∞ compensator design

The 21^{st} order system defined in Eq. (2) and Eq. (3) is considered here. Sensor-based joint position estimation is generally imprecise because of the presence of noise. An estimator algorithm from H_∞ control synthesis is generated, successfully stabilizing the proposed biomechanical model for the partially impaired hand in the presence of disturbances. The theoretical framework for the proposed model, together with the input process noise and the output measurement noise, is described in Eq. (5). The input noise $\vec{n}(t)$ and the output noise $\vec{v}(t)$ are defined in Eq. (6) and (7) respectively.

$$\dot{\vec{x}}(t) = A\vec{x}(t) + B_u\vec{u}(t) + B_w\vec{w}(t). \tag{5}$$

The vector $\vec{x}(t)$ and $\vec{u}(t)$ are as given in the previous section. Under the assumption of stationary white noise processes, the covariance matrices are written as:

$$E((n(t)n^T(t+\tau)) = S_n\delta(\tau) \tag{6}$$

$$E((v(t)v^T(t+\tau)) = S_v\delta(\tau) \tag{7}$$

The overall system, including measured and regulated variables, is given as matrix **M** as follows:

$$M = \begin{bmatrix} A & B_u & B_w \\ C_m & D_{mu} & D_{mw} \\ C_y & D_{yu} & D_{yw} \end{bmatrix}$$

In this study, various matrices are utilized to depict the dynamics and attributes of the partially impaired human hand model. Matrix A, an element of the vector space of real numbers $R^{21\times21}$, functions as the state matrix, representing the dynamics pertaining to the 21 states that characterize the hand's behavior. The column matrix B_u, also in $R^{21\times1}$, represents the input matrix and gives the single external voltage input used to mimic the muscle force supplied to the MCP joint of the robotic digit in our model. B_w is expanded to a size of $R^{21\times2}$ and is specifically allocated to accommodate external disturbances. These disturbances include both process noise and measurement noise.

In addition, matrices C_m ($R^{1\times21}$) and C_y ($R^{22\times21}$) are included in order to function as state optimization matrices. In a broad context, matrices D_{mu} ($R^{1\times1}$) and D_{yw} ($R^{22\times2}$) are initialized as matrices consisting entirely of zeros. When the value of D_{mu} is 0, it indicates the absence of any influence or contribution from the input signal $\vec{u}(t)$ on the measurement function. Furthermore, it is necessary for matrices D_{mw} ($R^{1\times2}$) and D_{yu} ($R^{22\times1}$) to preserve full row rank and full column rank, respectively. D_{mw} represents the disturbance applied to the measured output weighting function, whereas D_{yu} represents the input to the desired output weighting function.

By minimizing the H_∞-norm and solving algebraic Riccati equations (AREs), the H_∞ optimum controller is found. The measured and controlled outputs are given as:

$$\begin{bmatrix} m(t) \\ y(t) \end{bmatrix} = \begin{bmatrix} C_m \\ C_y \end{bmatrix} x(t) + \begin{bmatrix} D_{mu} & D_{mw} \\ D_{yu} & D_{yw} \end{bmatrix} \cdot \begin{bmatrix} u(t) \\ w(t) \end{bmatrix}$$

The AREs are given by Eq. (8) and Eq. (9). If a positive semi-definite solution exists for the formulated problem, then solving these two equations yields a steady-state solution. Let P and Q be the unique symmetric positive semi-definite solutions to the AREs for the H_∞ compensator formulation as given below:

$$PA + A^TP - P(B_uB_u^T - \gamma^{-2}B_wB_w^T)P + C_yC_y^T = 0 \tag{8}$$

$$AQ + QA^T - Q(C_m^TC_m - \gamma^{-2}C_y^TC_y)Q + +B_wB_w^T = 0 \tag{9}$$

The value of γ specifies the minimum acceptable bound on the estimation error and the input disturbance. The minimum bound for the linear model is found by using Eq. (10), which determines the spectral radii of Eq. (8) and Eq. (9).

$$\rho(PQ) < \gamma_i^2 \tag{10}$$

4.2. Minimum realization problem of the proposed model

According to Bart De Schutter in [53], the core challenge of the minimal realization problem in linear time-invariant (LTI) systems is to find a minimal state-space realization that includes specific information about these systems. The minimal realization possesses controllability and observability attributes, rendering it suitable for constructing an observer. This observer estimates system states based on output measurements, subsequently facilitating the development of a state feedback controller, as described in [54].

The matrices in our proposed model are considered a 4-tuple LTI system (A, B, C, D). This realization of (A, B, C, D) in state space has a full order of n equal to 21, where n is the number of states. The theorem ascribed to Kalman characterizes a minimal state space realization, which states that *"A realization (A, B, C, D) is minimal if and only if it is controllable and observable"*. The computational cost of optimizing controller parameters is reduced by transforming the augmented model into a distinct canonical formulation using a minimal realization technique.

There are two broad classes into which the minimal state space realization methods may be sorted. A minimum realization strategy emphasizes eliminating non-minimal realizations as given in [55]. In this research, Rosenbrock presents a methodical two-step approach for converting a state space realization of full order into its minimal realization model. The algorithm for minimum realization functions in the following manner: The matrices A, B, and C are combined into a single matrix, denoted as P.

$$P = \begin{bmatrix} A & B \\ C & 0 \end{bmatrix}$$

The matrix P is converted into a matrix $\hat{P}$ by performing a similarity transformation on it as given below:

$$\hat{P} = \begin{bmatrix} \bar{A}_{\bar{c}} & 0 & 0 \\ \bar{A}_{21} & \bar{A}_c & \bar{B}_c \\ \bar{C}_{\bar{c}} & \bar{C}_c & 0 \end{bmatrix} = \begin{bmatrix} \hat{A} & \hat{B} \\ \hat{C} & 0 \end{bmatrix}$$

Table 2
Close loop eigenvalues of the full order and minimal realization model.

full order Model	Minimal Realization Model
-0.1635 + 60.5491i	-0.1635 + 60.5491i
-0.1635 - 60.5491i	-0.1635 - 60.5491i
-33.2481 + 8.8815i	-33.2481 + 8.8815i
-33.2481 - 8.8815i	-33.2481 - 8.8815i
-35.3582 + 0.0000i	-35.3582 + 0.0000i
-18.5229 + 0.0000i	-18.5229 + 0.0000i
-5.5394 + 16.0166i	-5.5394 + 16.0166i
-5.5394 - 16.0166i	-5.5394 - 16.0166i
-10.4499 + 8.1127i	-10.4499 + 8.1127i
-10.4499 - 8.1127i	-10.4499 - 8.1127i
-6.2638 + 0.0000i	-6.2638 + 0.0000i
-1.4674 + 5.5368i	-1.4674 + 5.5368i
-1.4674 - 5.5368i	-1.4674 - 5.5368i
-0.7286 + 5.5259i	-0.7286 + 5.5259i
-0.7286 - 5.5259i	-0.7286 - 5.5259i
-1.0739 + 0.0000i	-1.0739 + 0.0000i
-0.0021 + 0.0000i	-0.0021 + 0.0000i
-0.0473 + 0.0000i	-0.0473 + 0.0000i
-1.4729 + 0.0000i	
-0.5726 + 5.5205i	
-0.5726 - 5.5205i	

where ($\bar{A}_c$, $\bar{B}_c$, $\bar{C}_c$, D) is controllable. Because of the similarity transformation that relates it to the given system, the set ($\hat{A}$, $\hat{B}$, $\hat{C}$, D) is also a realization. Furthermore, the state-space realization ($\bar{A}_c$, $\bar{B}_c$, $\bar{C}_c$, D) is a controllable realization of the provided system. Using a corresponding approach on the matrix Q given as:

$$Q = \begin{bmatrix} \bar{A}_c^T & \bar{A}_c^T \\ \bar{A}_c^T & 0 \end{bmatrix}$$

we obtain an observable realization of the form:

$$\hat{Q} = \begin{bmatrix} \bar{A}_{\bar{o}} & \bar{A}_{12} & \bar{B}_{\bar{o}} \\ 0 & \bar{A}_o & \bar{B}_o \\ 0 & \bar{C}_o & 0 \end{bmatrix}$$

where ($\bar{A}_o$, $\bar{B}_o$, $\bar{C}_o$, D) is observable. The resulting realization **M** is controllable, observable now, and minimal.

$$M = \begin{bmatrix} A & B_u & B_w \\ C_m & D_{mu} & D_{mw} \\ C_y & D_{yu} & D_{yw} \end{bmatrix}$$

Where A is an 18^{th} order matrix representing all the states of the plant that are controllable and observable. The rest of the matrices have been defined in the previous section. The states removed after the minimal realization are identified by Jordan decomposition. Table 2 gives the eigenvalues of the 21^{st} order and the 18^{th} order model.

The three states that are removed are $\overrightarrow{x_{19}}(t)$, $\overrightarrow{x_{20}}(t)$ and $\overrightarrow{x_{21}}(t)$. These states correspond to the mechanical displacement of stiffness element C_5 (MCP of the little finger), the momentum of inertia I_4 (MCP of the little finger) and the momentum of inertia element I_5 (MCP of the thumb). All the states of the anthropomorphic index finger are controllable and observable. Hence, the reduced order model can be simulated for robust tracking control so that the desired state achieves the equilibrium position in the minimum possible time that is physiologically relevant.

The control objectives for the minimum realization model represented by the matrix **M** consist of designing an efficient controller so that the closed-loop system will be asymptotically stable and the constraints will always be achieved over the control horizon. These two goals must be accomplished by adjusting the control input $\vec{u}(t)$ to direct the required state to the equilibrium point. In contrast, the control inputs are necessary to maintain a desirable range.

5. Reference trajectory and tracking control

The primary objective is to ensure that the output vector $\vec{y}(t)$ behaves as anticipated, even in the presence of various transient uncertainties inherent in the process. Specifically, when the reference signal $\vec{r}(t)$ remains consistent over time, the output $\vec{y}(t)$ should exhibit minimal overshoot and achieve rapid rise time. Meeting these performance criteria is essential to ensure that the output trajectory closely aligns with an ideal trajectory for $t \in [t_0, \infty)$, or in alternative terms, the limit as t approaches infinity should result in $|\vec{y}(t) - \vec{r}(t)| \to 0$.

This requirement underscores the need for precise and responsive control mechanisms to maintain the desired output behavior, even in the face of unpredictable fluctuations or disturbances within the system. Achieving a close correspondence between the output and reference signals over time is crucial for ensuring the system's stability, reliability, and effectiveness in fulfilling its intended function. Thus, meticulous attention to performance specifications and the continuous refinement of control strategies are imperative to meet the stringent demands of real-world applications.

5.1. Reference trajectory for PIP joint of finger

An essential part of our approach is the reference trajectory model that we use to create a reference position profile for the index finger's PIP joint. A crucial aspect of our methodology is verifying the alignment between the reference trajectory and the experimental trajectory, as outlined by Friedman in his research [56].

In the field of hand surgery, there is a consensus among experts that scientific evidence supports the idea that the movement trajectory of the fingertip closely resembles that of a logarithmic spiral during both flexion and extension motions. The aforementioned empirical observation has been extensively expounded upon in existing research, as given by Gupta [57] and Kamper [58], whose investigations have made substantial contributions to our knowledge of hand biomechanics.

Our study uses a mathematical formulation to define the reference trajectory of the PIP joint during index finger flexion and extension movements, as shown in Eq. (11):

$$\vec{\theta}_{ref}(t) = \vec{\theta}_i(t) + (\vec{\theta}_f(t) - \vec{\theta}_i(t)).\vec{\theta}_r(t) \tag{11}$$

Here, $\vec{\theta_i}(t)$ and $\vec{\theta_f}(t)$ denote the initial and final positions, respectively, relative to the angle of the PIP joint. Moreover, $\vec{\theta_r}(t)$ is characterized as a sigmoid function, strategically employed to generate the trajectory, graphically depicted in radians versus time in seconds), as detailed by Eq. (12).

$$\vec{\theta}_r(t) = \frac{1}{1 + e^{(-a(\theta - c))}} \tag{12}$$

The parameter values are carefully chosen as $a = 0.1$ and $c = 0$, ensuring physiological relevance to hand closure times of 1–1.5 sec. The reference trajectory model is simulated over a time span of 2 sec, aligning with the natural dynamics of hand movements. The initial position θ_i of the PIP joint is set at 0.28 rad, representing a flexion position that culminates in a final joint angular position of θ_f at 1 rad. This configuration is designed to achieve a desired angular velocity of 0 rad/sec at the culmination of the motion, thereby optimizing the trajectory for effective movement execution.

5.2. Tracking and control of angular position

In order to achieve the highest level of trajectory tracking performance, it is crucial for the trajectory tracking control system to successfully meet the demanding target of minimizing the positional tracking error to an infinitesimally small amount. The level of precision required is crucial in order to ensure that the angular displacement trajectory $\vec{\theta_3}(t)$ precisely matches the prescribed reference trajectory $\vec{\theta}_{ref}(t)$ over the whole period of the motion.

The compensator, a crucial control system component, plays a significant role in coordinating system modifications to minimize tracking errors efficiently. The compensator reacts to the error signal, which acts as the primary input for the control mechanism. The error signal encompasses the differences between the observed angular displacement trajectory and the intended reference trajectory, providing the necessary input for precise and immediate adjustments to the control system. The input to the compensator is the error signal as given by Eq. (13) below:

$$\vec{e}(t) = \vec{\theta}_{ref}(t) - \vec{\theta_3}(t) \tag{13}$$

The design aims to discover a controller that optimally reduces the ∞-norm. We solve this problem by developing a compensator that minimizes the H_∞-norm [59].

6. Simulation results with comparison analysis

The biomechanical model of the partially amputated hand is represented by a bond graph, which is then simulated using MATLAB/Simulink based on Fig. 1. Two controller schemes are created to analyze simulation outcomes for the model defined by Eq. (5). We compare the simulation results of the full and reduced biomechanical models when subjected to perturbations impacting both input and output. We want to stabilize the system's behavior using H_∞ control approach. By utilizing this control strategy, we aim to reduce the impact of disturbances and guarantee strong performance despite external disruptions. This analysis aims to determine the optimal compensator for the extensive five-finger biomechanical model. We will consider many aspects, such as settling time, flexion and extension angles, and feedback muscle force while ensuring compliance with physiological limitations.

In this section, we undertake an extensive evaluation of the tracking control's efficacy concerning joint angular position, a pivotal aspect in emulating the natural motion characteristics of a human finger accurately. Our primary objective is to ensure that the proposed technique facilitates seamless, jerk-free trajectories like those observed in natural finger movements. Achieving this goal necessitates meticulous design considerations to minimize potential harm during the motion of the finger. These considerations are

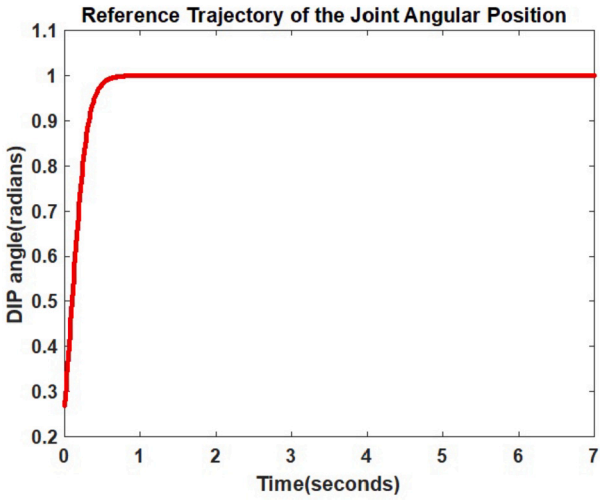

Fig. 2. Reference trajectory of the angular position of the PIP joint of the human index finger.

documented in the relevant literature [60]. By integrating insights from such studies, we aim to enhance the safety and authenticity of the proposed system's motion dynamics.

By conducting a thorough analysis and evaluation, our objective is to analyze how our compensator scheme contributes to achieving these desired features. This will result in a closer alignment of the system's behavior with the inherent movement patterns observed in natural human fingers.

The plot displayed in Fig. 2 illustrates the angular position profile of the PIP joint. This profile is an essential reference for the tracking control mechanism that governs the movement of the robotic index digit in our model framework. The profile, created using a sigmoid function, accurately depicts the angular position trajectory of the PIP joint, closely imitating the subtle motion patterns observed in a human index finger. This representation allows for a comprehensive understanding of how the movement of the robotic digit corresponds to the natural behavior of the human finger, providing vital insights into the efficiency and accuracy of our model's tracking control system.

In order to ensure the fidelity of this trajectory, we meticulously adjusted the parameters of the sigmoid function to closely mirror the trajectory obtained from experimental data, as outlined in [56]. The authors utilized forward kinematics to estimate angular displacements across various finger joints in their study. Notably, the initial joint angles in the experimental data display variability, influenced by factors such as initial conditions and the specific type of movement being analyzed. Consequently, these trajectories exhibit curved paths, eventually converging to an approximate value of 1 rad within a time frame ranging from 0.5 sec to 1 sec.

This approach enables us to replicate the natural trajectory of the PIP joint accurately, aligning our model's behavior with empirical observations from experimental studies. By adjusting the parameters of the sigmoid function to align with the actual data, we guarantee that our model accurately represents the specific movement patterns demonstrated by the human index finger. This level of precision enhances the authenticity and reliability of our model, thereby strengthening its utility for a wide range of applications in robotics and biomechanics research.

The tracking control trajectory in our model begins at an initial angular position of 0.28 rad and extends over 2 sec to reach a final position of 1 rad. The trajectory replicates the movement of a human finger, guaranteeing that the robotic finger's motions follow physiological limitations. Using this reference trajectory allows us to evaluate the stability of the robotic finger's movement while adhering to the physiological constraints seen in human fingers. This research allows us to draw significant parallels between the flexion and extension motions of the robotic index finger and those of a real human finger. The simulation results, presented within the palm-centered frame of reference, offer valuable insights into the performance of our robotic finger model.

In Fig. 3, it can be observed that the commencing angular velocity is recorded as 0.035 rad/sec as the finger begins its flexion movement in accordance with the reference trajectory illustrated in Fig. 2. The observed result has notable physiological significance, as it corresponds to the inherent speed properties of the PIP joint of the index finger, as evidenced by previous research conducted by Darling et al. [61] and Chen et al. [51]. The insight gained from this observation contributes to a deeper understanding of finger movement dynamics, especially in scenarios involving slower movements, which are integral to tasks requiring precision and control.

Moreover, Fig. 4 provides a visual representation of the angular position profile of the PIP joint, as predicted by our proposed model. The joint is transitioning from an initial angular position of 0.28 rad to a terminal position of 1 rad. The stabilization of motion occurs at approximately 6 sec, highlighting the dynamic nature of finger movements. This detailed analysis offers valuable insights into the kinematic behavior of the index finger's PIP joint, which is essential for developing accurate simulation models and enhancing our understanding of human motor control.

As supported by research conducted by [50,51], the PIP joint of the human index finger commonly has a range of motion between 0–1.92 rad, encompassing both extension and flexion movements. It is essential to acknowledge that the modification of the state weighting matrix C_y and the input weighting matrix D_{yu} inside the control design framework, as specified in matrix **M**, has a

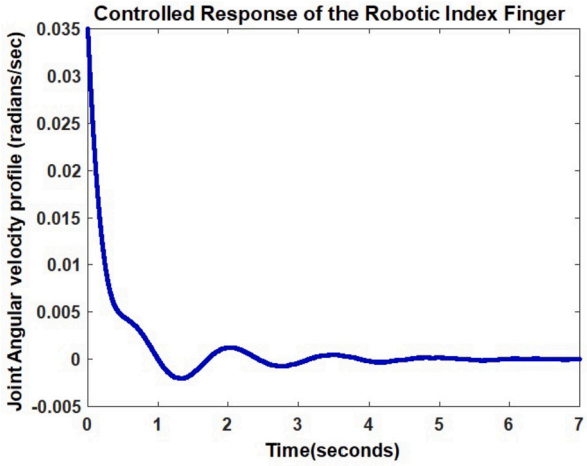

Fig. 3. Angular velocity profile of the PIP joint after the application of the H_∞ control scheme to full order model.

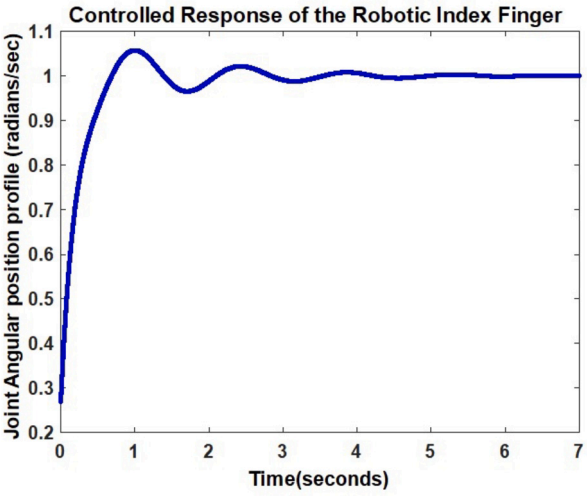

Fig. 4. Angular position profile of the PIP joint after the application of the H_∞ control scheme to full order model.

substantial effect on reducing the steady-state settling time. However, it is crucial to recognize that these modifications may require a higher level of input force. However, the outcomes of our simulation align with the physiological restrictions imposed by the human hand.

The observations mentioned above provide strong evidence for the accuracy and biological significance of our simulation results, demonstrating a comprehensive comprehension of the intricacies involved in human hand movements.

Fig. 5 represents the feedback force generated by the H_∞ controller. This force response is a direct outcome of the full order plant model simulation, a scenario encompassing additional uncertainties and disturbances within the system. In this context, the feedback force is a critical indicator of the controller's effectiveness in mitigating the impact of uncertainties and disturbances on the system's behavior. Analyzing this force profile helps assess the controller's ability to maintain stability, regulate the system's motion, and ensure that it adheres to the desired trajectory despite external factors that could disrupt its performance.

In conditions where external forces do not impede the natural motion of the finger, the influence of the compensator on the feedback force profile remains minimal. As the finger's movement unfolds, typically initiating from an extended position and concluding with a flexed posture, there is a discernible augmentation in the force exerted on the joint. This incremental increase in force facilitates the gradual transition of the finger from one state to another. Once the motion reaches a stable equilibrium point, typically representing the intended position, the feedback response returns to its baseline, effectively reaching a steady-state condition. This phenomenon shows that the CNS has managed a well-coordinated process. The CNS is crucial in controlling the finger's mobility, moving it from an initial state of disruption or rest to a precise and controlled ultimate position frequently seen at the PIP joint. It is important to note that the feedback force profiles are employed to establish the direction and amount of the forces, with positive values denoting extension forces and negative values denoting flexion forces.

The complex interaction among the compensator, feedback forces, and CNS control emphasizes the remarkable flexibility and precision inherent in the motion control system of the human hand. Gaining insights into these intricate dynamics holds critical

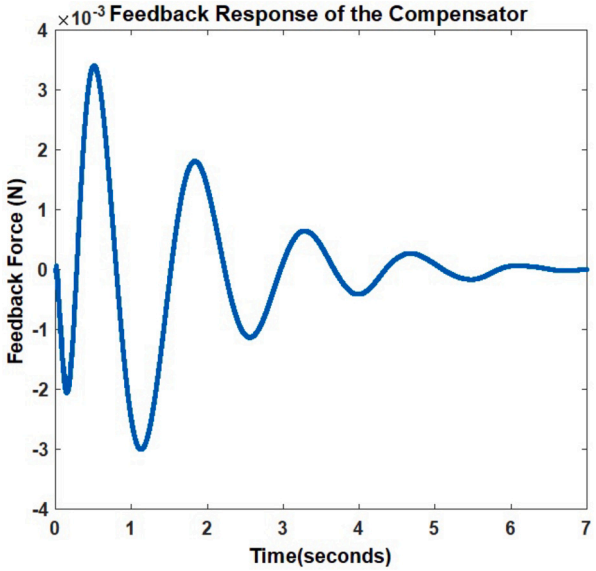

Fig. 5. Feedback force at the PIP joint of Robotic finger after the application of the H_∞ control scheme to full order model.

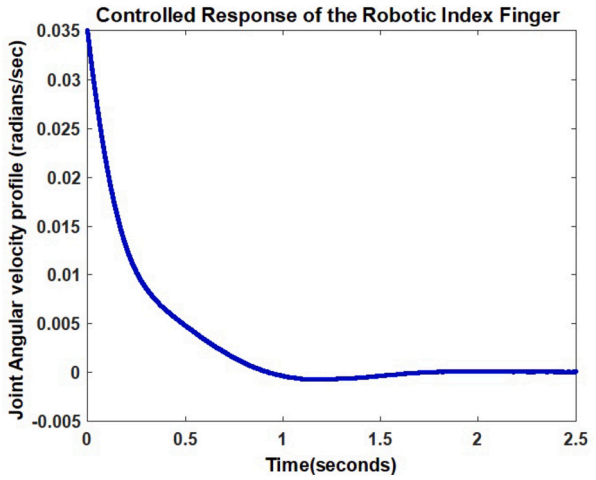

Fig. 6. Angular velocity profile of the PIP joint of the Robotic finger after the application of the H_∞ control scheme to a minimal realization model.

significance, not only in biomechanics but also in advancing sophisticated robotic systems aspiring to emulate the dexterity and control characteristic of a human hand motion.

Now, the reduced order model presented by matrix **M** is simulated for comparison with the simulation results of a full order model by employing the H_∞ robust and optimal control scheme. Fig. 6, Fig. 7 and Fig. 8 represent the angular velocity, angular position and compensator response of standard H_∞ control scheme applied to a minimal realization model.

When the finger is perturbed from an initial equilibrium position of 0.28 rad and an angular velocity of 0.035 rad/sec, it achieves the final desired equilibrium position of 1 rad within a time duration of 2 sec. The simulation results demonstrate the physiological relevancy of the proposed minimal realization model with the natural human hand physiological constraints. The compensator response in the form of the feedback control signal is depicted in Fig. 8, which is also within the bounds imposed by the physiological constraints of a human hand.

The control of joint angular positions in the full order model is depicted in Fig. 9, showcasing the application of H_∞ control. At the outset, the angular displacement of both the reference trajectory and the PIP joint trajectory of the robotic index finger are similar. Furthermore, it demonstrates the plant's control reaction when the combined DIP and PIP joints of the robotic index finger experience an initial deflection of 0.28 rads. In the simulation, the system's response reaches a stable state at approximately 6 sec, while the tracking error gradually diminishes and approaches zero. The simulation findings presented in this study demonstrate the effective implementation of a robust controller for a hand with partial impairment consisting of five digits. However, the controller parameters do not conform to the inherent limitations imposed by the human hand.

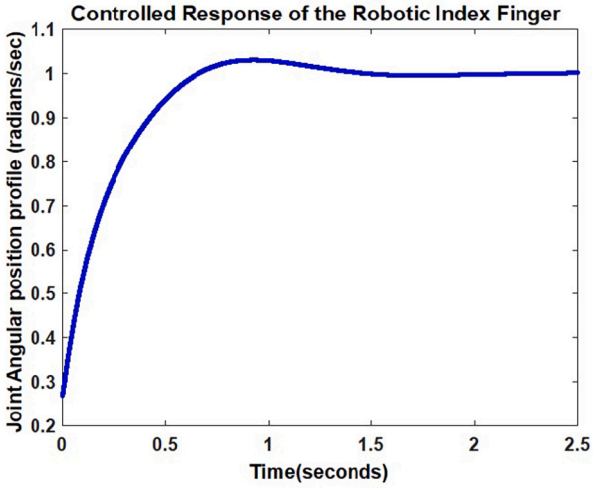

Fig. 7. Angular position profile of the PIP joint of the Robotic finger after the application of the H_∞ control scheme to minimal realization model.

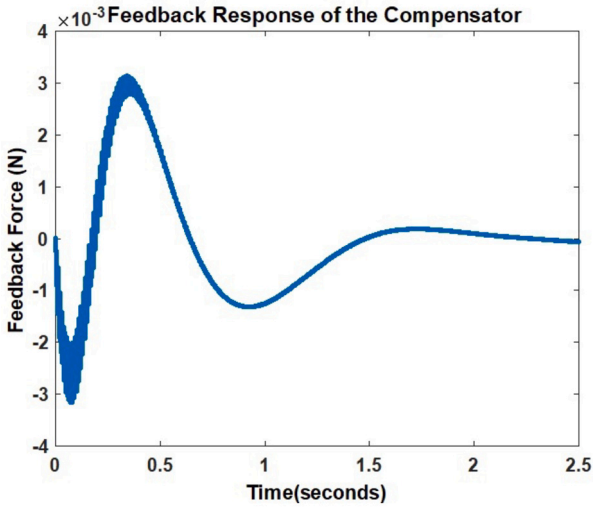

Fig. 8. Feedback force at the PIP joint of Robotic finger after the application of the H_∞ control scheme to minimal realization model.

Fig. 10 demonstrates the tracking control response of the minimal state space realization plant when the combined DIP and PIP joints of the robotic index finger have an initial deflection of 0.28 rad. The response stabilizes at approximately 2 sec in simulation time. All the minimally realized model states are fully stable after applying an H_∞ controller scheme.

Hence, the reference trajectory is used to create a feedback force at the CNS. The plot shows that the proposed control approach can keep the finger on track with the reference trajectory even when some unknown perturbation is present. The robustness and capacity to sustain effective tracking performance of the control scheme are showcased here. The PIP joint's angular position profile shows an early peak in the joint angle, suggesting a sudden jerk in the finger movement. This is followed by recurrent oscillations until the joint reaches equilibrium. Therefore, it can be inferred that the accuracy of trajectory tracking for a minimal order plant using the proposed H_∞ control method is significantly higher than that for the full order model using the same control method. Furthermore, we show that all signals in the closed-loop system are equally limited by the suggested control method for angular position monitoring. Position tracking errors can also converge to a small, desirable quantity if the design parameters are chosen correctly.

The evaluation of the robust performance of the suggested model in addressing the issue of trajectory tracking offers substantiation for the efficacy and significance of the approach. The estimation of actuation force in relation to the PIP joint trajectory was achieved by including a feedback signal from the controller. Determining actuation force is of utmost importance as it enables the model to replicate the observed biological muscle function involved in coordinating finger movements. The aim of reproducing this mechanism in force actuation at the phalanges is to attain coordination and movement patterns that closely resemble the natural hand functions observed in humans while ensuring robust tracking control.

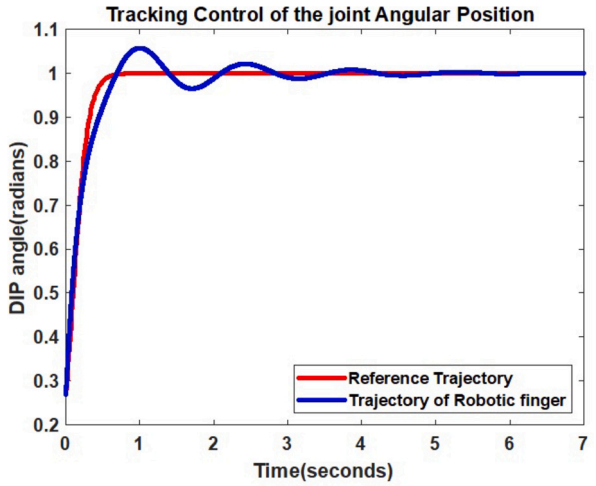

Fig. 9. H_∞ tracking control of the trajectory of the PIP joint of a full order model.

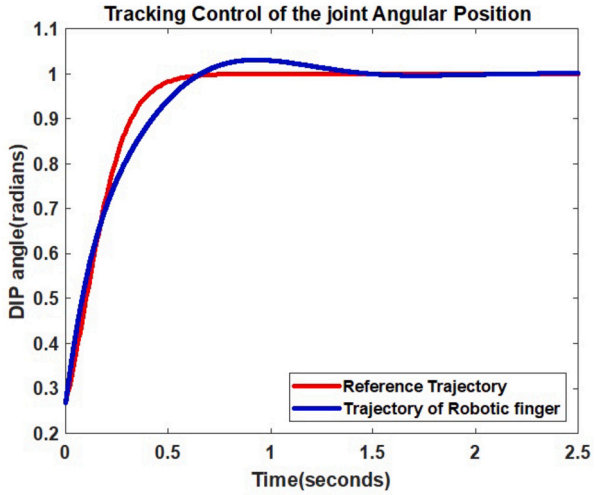

Fig. 10. H_∞ tracking control of the trajectory of the PIP joint of a minimal realization model.

Table 3
Comparison of the full order & minimal realization responses.

Plant Response Parameter	Full Order System	Minimal Realization System
Peak Overshoot	Overshoots to 1.05 rad	Overshoots to 1.02 rad
Settling Time	Stabilizes at 6 sec	Stabilizes at 2 sec
Disturbances	Initial oscillatory behavior	Negligible jitters
γ value achieved	1.09	1.06

7. Performance analysis of H_∞ control scheme for full order and minimal order model

In this section, an analysis is conducted on the simulation results of the full order biomechanical model, comparing it to the minimally realized model in the presence of input and output disturbances. The system's response was stabilized by employing an H_∞ control method.

A 21^{st} order model describes the impaired hand's full order biomechanical system. After compensating with H_∞ control scheme, it has 21 stable states, indicating that the full order model is stabilizable and detectable. After minimally realizing the full order state space model, an 18^{th} order system is achieved that is fully controllable and observable. The system's responses were completely stable when the H_∞ compensator was developed. Table 3 compares the results of the two simulations.

The response of both controllers differs in terms of steady-state settling time, overshoot and trajectory of flexion angles. The findings show that the plant response exhibits earlier stabilization once we have implemented the minimal state space realization,

Table 4
Comparison of the PIP joint angular position profile of the proposed H_∞ control framework with experimental research work.

Comparison parameter	Proposed H_∞ control	Experimental results [56]	Experimental results [62]
Methodology Implemented	Simulation of a biomechanical model in MATLAB/Simulink	Wearable CyberGlove	Exoskeleton
Initial PIP joint angle	0.28 rad	0.42 rad	0.349 rad
Final achieved PIP joint angle	1 rad	1 rad	1.08 rad
Settling Time	1 sec	1 sec	4 sec
Path followed by the Trajectory	Sigmoid Function	Sigmoid Function	Sigmoid Function

aligning it closely with the actual model. Furthermore, the minimal realization model establishes a more stringent lower limit, denoted as γ, on both disturbance input and estimation error compared to the full order model.

These outcomes demonstrate the successful development of a stable controller designed for the partially impaired human hand model with five digits. This achievement highlights the effectiveness of the minimal realization approach in enhancing stability and control performance within the system.

7.1. Comparison with experimental data

In this section, we will conduct an empirical validation by carefully examining and comparing the simulated results obtained from our model. Our focus revolves around the joint angular position profile and its conformity to observed motion dynamics in the index finger. This comparative analysis incorporates the essential insights derived from the works of [56] and [62], wherein the intricate interplay between the CNS input and finger movements was methodically explored.

Additionally, we broaden our analysis to encompass the Range of Motion (RoM) about the PIP joint of our anthropomorphic index finger model. This expansion requires a careful juxtaposition with experimental investigations, as illustrated in scholarly initiatives published by Jo et al. [63] and Yang et al. [64]. These researchers investigated the kinetics of flexion and extension of the human hand. A thorough understanding of finger kinematics was provided by the experimental protocol defined by Friedman et al. [56]. This protocol was characterized by wearable CyberGlove technology, which made it possible to track joint angles meticulously. Seven volunteers, with a mean age of 31, were engaged in gripping actions while joint angles were measured at a rate of 90 Hz. Utilizing forward kinematics simplified the process of determining the angular displacements of every finger joint, enabling a comprehensive examination of finger motions. When grabbing something, the fingers open up a bit before wrapping around it. Because of this, it is possible to conduct comparison evaluations under different starting conditions, like different index finger flexion motions.

The simulation results provide a comprehensive view of our exploratory activities, which are displayed within the context of the frame of reference that is fixed in the palm. Fig. 2 provides a visual representation of the angular position profile at the PIP joint, which has a central position in our analytical discourse. The precision that is inherent in our modeling technique is highlighted by the delineation of the beginning angular location, which was calibrated at 0.28 rad and gradually transitioned to a culmination at 1 rad over the course of a stabilization phase that lasted approximately 1 sec.

Furthermore, our empirical data from experimental trials revolve around gripping dynamics, which were rigorously investigated from the perspective of the object's frame of reference. These empirical observations reveal an angular displacement trajectory of the index finger. The trajectory begins with an initial position that is approximately 0.42 rad and culminates in a flexion angle of 1 rad within a temporal period of 0.5 sec.

Fig. 10 visually represents joint angular position tracking control. It integrates H_∞ control smoothly, an essential aspect of our academic investigation. The first angular perturbation, which begins at 0.28 rad and mirrors our a priori specifications, is precisely staged, and the controller demonstrates an exceptional level of fidelity in tracking the reference trajectory within a brief time gap of the equivalent of 2.5 sec.

We provide evidence to support our simulation results by doing a comprehensive comparative study with the experimental findings thoroughly documented by Kakoty et al. [62]. In the experimental paradigm, finger trajectories were methodically captured by a finger exoskeleton equipped with position sensors. The experiment involved sixteen subjects participating in four finger flexion and extension sessions. To determine whether or not the outcomes of our simulation are accurate, this empirical corpus acts as a pivot point.

The angular position profile of the PIP joint, as instantiated in our proposed model, demonstrates remarkable congruence with the observed profile that was outlined in the experimental simulations that were elaborated upon by Kakoty et al. [62]. This becomes apparent becomes evident upon careful examination. The scholarly rigor that underpins our anthropomorphic index finger model is highlighted by this corroboration, which serves as a convincing testimonial to the fidelity that is inherent in the outcomes of our simulation. The tabular synthesis shown in Table 4 offers a succinct summary of our comparative analysis, enhancing the validity of our academic research.

In conclusion, an examination is conducted to compare the RoM exhibited by the PIP joint of the index finger within our proposed model (Table 5) with the RoM observed in experimental studies documented in [63,64].

8. Discussion and conclusion

Incorporating coordination with the CNS into the biomechanical model of a disabled hand poses significant challenges for modeling and controlling an anthropomorphic hand with partial impairment. Our model, representing five digits, underwent analysis using

Table 5
Comparison of the RoM of the PIP joint of the index finger of the proposed H_∞ controller framework with experimental work.

Comparison parameter	H_∞ controller	Experimental results [65]	Experimental results [64]
Joint name	Combined PIP-DIP joint	PIP joint	PIP joint
Motion of index finger	Flexion	Flexion-Relaxation-Extension	Flexion-Extension
Range of motion (RoM)	0.28–1 rad	0–1.85 rad	0–1.92 rad

Table 6
Performance comparison of the proposed minimal realized H_∞ control framework with current research work.

Comparison parameter	Proposed H_∞ control	[66] ESO+ SMC Control	[67] PD Control	[68] Feedback Linearization Control
Function	Flexion	Flexion	Flexion	Flexion
Maximum achieved PIP joint angle	1 rad	0.26 rad	0.35 rad	0.78 rad
Disturbance Rejection	Yes	Yes	No	No
Settling Time	1 sec	20 sec	30 sec	5.5 sec

a bond graph modeling approach. We utilized a CNS model as an optimal controller, denoted as H_∞, to synchronize the actions of both artificial and human fingers.

The original state space model is of 21^{st} order, but it was reduced to an 18^{th} order model. The resulting model states were fully observable and controllable. Through the development of a minimal realization model, we were able to evaluate the stability of both systems in relation to each other.

A state feedback controller was formulated, and computational complexity was mitigated by transforming the full order model into a minimal realization formulation. To account for noisy joint sensor data physiologically, noise and disturbance were integrated into the model.

In our investigation, Simulink was utilized to simulate the model, enabling us to evaluate its performance under disturbances and stochastic processes associated with measurement noise. To effectively coordinate and control the proposed model, a controller synthesis strategy was devised employing the H_∞ control algorithm. The primary aim of this control approach was to achieve the desired system response in minimal time while minimizing the effects of disruptions. The selection of the minimal realization of the model is particularly noteworthy due to its advantageous characteristics in observability and controllability. This minimal realization lays the groundwork for the development of an observer, essential for estimating a system's states using output measurements and the control signal provided by a state feedback controller. Furthermore, our control framework utilizes the feedback signal from the controller to estimate the actuation force concerning the trajectory of the PIP joint, a crucial step in ensuring precise and coordinated system control, thus enhancing its effectiveness and reliability.

The function of biological muscles responsible for coordinating finger motions is replicated through force actuation at the phalanges. A reference trajectory is generated using the sigmoid function, with the angular velocity and displacement profiles of the index finger accurately reflecting those of a human index finger.

The angular position profile stabilizes at 1 rad within a time of 2 sec, marking the culmination of the motion from an extended to a flexed position. At the movement's onset, the compensator response within the feedback force profile is zero, indicating motion initiation without external force. As the motion progresses, force gradually accumulates, aiding the transition to the flexed state. Ultimately, the response returns to its initial zero value, achieving equilibrium.

Our simulation results demonstrate a consistent and stable response well within physiological boundaries. Various factors, including disturbances and joint sensor noise and inherent challenges in real-world scenarios, are considered in this research. Recognizing that achieving higher physiological relevance may entail a more thorough exploration of parametric variables within the model is crucial. This aspect suggests a potential avenue for future research. Expanding the modeling effort as proposed could offer several benefits, including improved settling time, enhanced disturbance rejection, and reduced tracking control errors.

Our simulation results underscore significant attributes, such as enhanced settling time, heightened capability to reject disturbances, and diminished tracking control errors. These observations underscore the potential of the proposed model to emulate the physiological dynamics of human motion. Table 6 provides a comparative analysis between our research and existing studies that integrated disturbances and modeling uncertainties into their models. This study conducts comparative research on various aspects concerning the movement profiles of the PIP joint.

Maintaining a flexion angle range of 1.92 rad at the PIP joint is essential for achieving physiologically accurate index finger movement. Additionally, it is crucial that the time required to reach a stable equilibrium position for the angular position profile of the joint does not exceed the physiological limit of 1.5 sec.

Parameters relevant for assessing the angular position profile of the mechanical PIP joint encompass the final steady-state position, peak response, ability to counteract external perturbations, and time needed to achieve stability. Based on the data presented in Table 6, it can be inferred that our study's control methodology demonstrates superior performance concerning settling time compared to the simulation outcomes reported in [66–68].

Zhao et al. [66] presents a sliding mode controller integrated with an extended state observer to address nonlinearities and disturbances in a two-joint coupling finger mechanism. The controller demonstrates commendable performance in disturbance rejection;

however, its settling time of 20 sec does not align with the natural settling time observed in the trajectory of the PIP joint in a human finger.

Ali et al. [67] developed a biomimetic mechanism to emulate human finger characteristics. Utilizing the existing mathematical model, they designed a PD controller to manipulate the finger mechanism. While achieving a stable position at 30 sec, their approach lacks adequate disturbance rejection capability.

In a recent study, Alam et al. [68]) introduce an innovative quasi-static model-based control method to manage the motion of a soft robotic exo-digit effectively. Their approach employs input-output feedback linearization to linearize interconnections among various elements within the exo-digit. Although the proposed control mechanism exhibits stability, it requires an extended duration of 15 sec to achieve stability, which contradicts physiological principles. Furthermore, the method demonstrates limitations in effectively rejecting external disturbances.

Our simulation approach demonstrates robustness and stability within the palm frame of reference, addressing physiological constraints. Additionally, our control paradigm effectively mimics the functionality of the central nervous system in the human body.

The study of implementing minimal state space in Linear Time-Invariant (LTI) systems is crucial due to its simplification of complex problems, such as dealing with noisy inputs and nonlinear models. It serves as a foundation in system theory, providing insights into more intricate issues. Reducing the order of a controller facilitates comparative assessments of stability responses against minimal realization-based models, making designs more practical and cost-effective.

However, there are limitations to the proposed model. Reducing the mathematical model's order may lead to a loss of subtleties in impaired hand behavior, reducing precision in forecasting specific impairments. The effectiveness of reduced models depends on the complexity of the disability being simulated. Future work could involve simultaneous consideration of movement coordination in natural and robotic digits, expanding the scope of the study.

Funding

The authors did not receive any funding for this research.

CRediT authorship contribution statement

Maryam Iqbal: Conceptualization, Methodology, Software, Validation, Writing – original draft, Writing – review & editing. **Junaid Imtiaz:** Formal analysis, Writing – review & editing. **Asif Mahmood:** Formal analysis, Supervision.

Declaration of competing interest

The authors declare that they have no known competing financial interests or personal relationships that could have appeared to influence the work reported in this paper.

Data availability

Data will be made available on request.

Appendix A. The basics of bond graphs

At its essence, bond graph formulation aims to identify and delineate the power sources and consumers within a system. One method to achieve this is by decomposing a physical system into its constituent elements. These elements are broadly categorized into three types: 1-port, 2-port, and multi-port components. It is crucial to note that the number of ports and physical connections an element possesses are directly correlated.

Two generalized variables, flow ($\mathbf{f}(t)$) and effort ($\mathbf{e}(t)$), characterize any dynamic system in bond graphs. The power relayed between components is represented by the product of these variables, which reflects their interrelationships. While mechanical systems link flow and effort to quantities like force and velocity, electrical systems relate them to characteristics like voltage and current.

Both momentum ($\mathbf{p}(t)$) and position ($\mathbf{q}(t)$) are examples of energy variables, alongside power variables. The following equations provide the definitions of these terms, which are the time integrals of effort and flow, respectively:

$$\mathbf{p}(t) = \int \mathbf{e}(t) \tag{A.1}$$

$$\mathbf{q}(t) = \int \mathbf{f}(t) \tag{A.2}$$

Using the energy variables, the power variables can be derived as follows:

$$\mathbf{e}(t) = \dot{\mathbf{p}}(t) \tag{A.3}$$

$$\mathbf{f}(t) = \dot{\mathbf{q}}(t) \tag{A.4}$$

Bond graph elements can be single, two, or multi-port components. Examples include resistance (**R-elements**), inertia (**I-elements**), capacity (**C-elements**), and ideal sources of effort and flow. The functional relationships between effort and flow variables for these elements are expressed through equations.

Ideal sources of effort and flow are efficient power generators in bond graphs. They exhibit characteristics where the flow (or effort) depends solely on time and remains independent of effort (or flow). Transducers, portrayed as 2-port components, enable bidirectional energy transmission between ports and encompass various devices like transformers and electric motors. Ideal transducers assume zero power dissipation and a linear relationship between input and output signals.

The loss-less assumption simplifies the analysis, resulting in two types of transducers: transformers and gyrators. Transformers establish a connection between flow or effort variables, while gyrators exhibit a direct proportionality between these variables, determined by the transformer and gyrator modulus.

Multi-port elements, like transducers, conserve energy. There are two types: the 0-junction and the 1-junction. In a 0-junction, exerted efforts are equal, and the combined sum of flows is zero. Conversely, in a 1-junction, flows are uniform, and the combined sum of efforts is zero, akin to Kirchhoff's voltage law in electrical circuits and Newton's second law in mechanical systems.

References

[1] F.J. Valero-Cuevas, F.E. Zajac, C.G. Burgar, Large index-fingertip forces are produced by subject-independent patterns of muscle excitation, J. Biomech. 31 (8) (1998) 693–703.

[2] E.J. Earley, L.J. Hargrove, T.A. Kuiken, Dual window pattern recognition classifier for improved partial-hand prosthesis control, Front. Neurosci. 10 (2016) 58.

[3] I. Imbinto, C. Peccia, M. Controzzi, A.G. Cutti, A. Davalli, R. Sacchetti, C. Cipriani, Treatment of the partial hand amputation: an engineering perspective, IEEE Rev. Biomed. Eng. 9 (2016) 32–48.

[4] G.-C. Jeong, Y. Kim, W. Choi, G. Gu, H.-J. Lee, M.B. Hong, K. Kim, On the design of a novel underactuated robotic finger prosthesis for partial hand amputation, in: 2019 IEEE 16th International Conference on Rehabilitation Robotics, ICORR, IEEE, 2019, pp. 861–867.

[5] E.D. Engeberg, A physiological basis for control of a prosthetic hand, Biomed. Signal Process. Control 8 (1) (2013) 6–15.

[6] G.P. Kontoudis, M. Liarokapis, K.G. Vamvoudakis, A compliant, underactuated finger for anthropomorphic hands, in: 2019 IEEE 16th International Conference on Rehabilitation Robotics, ICORR, IEEE, 2019, pp. 682–688.

[7] C.-H. Chen, D.S. Naidu, Hybrid control strategies for a five-finger robotic hand, Biomed. Signal Process. Control 8 (4) (2013) 382–390.

[8] A. Prakash, A.K. Sahi, N. Sharma, S. Sharma, Force myography controlled multifunctional hand prosthesis for upper-limb amputees, Biomed. Signal Process. Control 62 (2020) 102122.

[9] T. Tuncer, S. Dogan, A. Subasi, Novel finger movement classification method based on multi-centered binary pattern using surface electromyogram signals, Biomed. Signal Process. Control 71 (2022) 103153.

[10] Q. Luo, C.M. Niu, J. Liu, C.-H. Chou, M. Hao, N. Lan, Evaluation of model-based biomimetic control of prosthetic finger force for grasp, IEEE Trans. Neural Syst. Rehabil. Eng. 29 (2021) 1723–1733.

[11] D. Farina, N. Jiang, H. Rehbaum, A. Holobar, B. Graimann, H. Dietl, O.C. Aszmann, The extraction of neural information from the surface EMG for the control of upper-limb prostheses: emerging avenues and challenges, IEEE Trans. Neural Syst. Rehabil. Eng. 22 (4) (2014) 797–809.

[12] B. Siciliano, O. Khatib, T. Kröger, Springer Handbook of Robotics, vol. 200, Springer, 2008.

[13] S.-H. Cha, T. Lasky, S. Velinsky, Determination of the kinematically redundant active prismatic joint variable ranges of a planar parallel mechanism for singularity-free trajectories, Mech. Mach. Theory 44 (5) (2009) 1032–1044, https://doi.org/10.1016/j.mechmachtheory.2008.05.010.

[14] B. Cai, Y. Zhang, Equivalence of velocity-level and acceleration-level redundancy-resolution of manipulators, Phys. Lett. A 373 (38) (2009) 3450–3453, https://doi.org/10.1016/j.physleta.2009.07.045.

[15] W. Wiedmeyer, P. Altoé, J. Auberle, C. Ledermann, T. Kröger, A real-time-capable closed-form multi-objective redundancy resolution scheme for seven-DoF serial manipulators, IEEE Robot. Autom. Lett. 6 (2) (2020) 431–438.

[16] U. Trivedi, D. Menychtas, R. Alqasemi, R. Dubey, Biomimetic approaches for human arm motion generation: literature review and future directions, Sensors 23 (8) (2023) 3912, https://doi.org/10.3390/s23083912.

[17] Y. Zhang, Z. Tan, K. Chen, Z. Yang, X. Lv, Repetitive motion of redundant robots planned by three kinds of recurrent neural networks and illustrated with a four-link planar manipulator's straight-line example, Robot. Auton. Syst. 57 (6–7) (2009) 645–651, https://doi.org/10.1016/j.mechatronics.2008.04.005.

[18] M.D. Fiore, G. Meli, A. Ziese, B. Siciliano, C. Natale, A general framework for hierarchical redundancy resolution under arbitrary constraints, IEEE Trans. Robot. (2023).

[19] A. Ghosal, Resolution of redundancy in robots and in a human arm, Mech. Mach. Theory 125 (2018) 126–136, https://doi.org/10.1016/j.mechmachtheory.2017.12.008.

[20] J. Lin, Y. Wu, T.S. Huang, Modeling the constraints of human hand motion, in: Proceedings Workshop on Human Motion, IEEE, 2000, pp. 121–126.

[21] A.M. Zanchettin, L. Bascetta, P. Rocco, Achieving humanlike motion: resolving redundancy for anthropomorphic industrial manipulators, IEEE Robot. Autom. Mag. 20 (4) (2013) 131–138.

[22] F. Flacco, A. De Luca, O. Khatib, Control of redundant robots under hard joint constraints: saturation in the null space, IEEE Trans. Robot. 31 (3) (2015) 637–654.

[23] J. Xiang, C. Zhong, W. Wei, A varied weights method for the kinematic control of redundant manipulators with multiple constraints, IEEE Trans. Robot. 28 (2) (2011) 330–340.

[24] J. Wan, H. Wu, R. Ma, L. Zhang, A study on avoiding joint limits for inverse kinematics of redundant manipulators using improved clamping weighted least-norm method, J. Mech. Sci. Technol. 32 (2018) 1367–1378, https://doi.org/10.1007/s12206-018-0240-7.

[25] H. Su, N. Enayati, L. Vantadori, A. Spinoglio, G. Ferrigno, E. De Momi, Online human-like redundancy optimization for tele-operated anthropomorphic manipulators, Int. J. Adv. Robot. Syst. 15 (6) (2018) 1729881418814695, https://doi.org/10.1177/1729881418814695.

[26] S. Li, K. Han, P. He, Z. Li, Y. Liu, Y. Xiong, Human-like redundancy resolution: an integrated inverse kinematics scheme for anthropomorphic manipulators with radial elbow offset, Adv. Eng. Inform. 54 (2022) 101812, https://doi.org/10.1016/j.aei.2022.101812.

[27] A. Shafei, H. Mirzaeinejad, A novel recursive formulation for dynamic modeling and trajectory tracking control of multi-rigid-link robotic manipulators mounted on a mobile platform, Proc. Inst. Mech. Eng., Part I, J. Syst. Control Eng. 235 (7) (2021) 1204–1217, https://doi.org/10.1177/0959651820973900.

[28] S.A. Kumar, R. Chand, R.P. Chand, B. Sharma, Linear manipulator: motion control of an n-link robotic arm mounted on a mobile slider, Heliyon (2023) e12867, https://doi.org/10.1016/j.heliyon.2023.e12867.

[29] V. Mata, S. Provenzano, F. Valero, J. Cuadrado, Serial-robot dynamics algorithms for moderately large numbers of joints, Mech. Mach. Theory 37 (8) (2002) 739–755, https://doi.org/10.1016/S0094-114X(02)00030-7.

[30] A. Agarwal, S. Shah, S. Bandyopadhyay, S. Saha, Dynamics of serial kinematic chains with large number of degrees-of-freedom, Multibody Syst. Dyn. 32 (2014) 273–298, https://doi.org/10.1007/s11044-013-9386-3.

[31] G. Gulletta, W. Erlhagen, E. Bicho, Human-like arm motion generation: a review, Robotics 9 (4) (2020) 102, https://doi.org/10.3390/robotics9040102.

[32] H. Kim, Z. Li, D. Milutinović, J. Rosen, Resolving the redundancy of a seven DOF wearable robotic system based on kinematic and dynamic constraint, in: 2012 IEEE International Conference on Robotics and Automation, IEEE, 2012, pp. 305–310.
[33] W. Liu, D. Chen, J. Steil, Analytical inverse kinematics solver for anthropomorphic 7-DOF redundant manipulators with human-like configuration constraints, J. Intell. Robot. Syst. 86 (2017) 63–79, https://doi.org/10.1007/s10846-016-0449-6.
[34] Y. Kadowaki, T. Noritsugu, M. Takaiwa, D. Sasaki, M. Kato, Development of soft power-assist glove and control based on human intent, J. Robot. Mechatron. 23 (2) (2011) 281–291, https://doi.org/10.20965/jrm.2011.p0281.
[35] P. Polygerinos, Z. Wang, K.C. Galloway, R.J. Wood, C.J. Walsh, Soft robotic glove for combined assistance and at-home rehabilitation, Robot. Auton. Syst. 73 (2015) 135–143, https://doi.org/10.1016/j.robot.2014.08.014.
[36] U. Jeong, H. In, H. Lee, B.B. Kang, K.-J. Cho, Investigation on the control strategy of soft wearable robotic hand with slack enabling tendon actuator, in: 2015 IEEE International Conference on Robotics and Automation, ICRA, IEEE, 2015, pp. 5004–5009.
[37] R.C. Luo, B.-H. Shih, T.-W. Lin, Real time human motion imitation of anthropomorphic dual arm robot based on Cartesian impedance control, in: 2013 IEEE International Symposium on Robotic and Sensors Environments, ROSE, IEEE, 2013, pp. 25–30.
[38] M. Alibeigi, S. Rabiee, M.N. Ahmadabadi, Inverse kinematics based human mimicking system using skeletal tracking technology, J. Intell. Robot. Syst. 85 (2017) 27–45, https://doi.org/10.1007/s10846-016-0384-6.
[39] M. Iqbal, A. Mahmood, Bond graph modeling and LQR control synthesis of a robotic digit in human impaired hand for anthropomorphic coordination, in: 2019 International Conference on Robotics and Automation in Industry, ICRAI, IEEE, 2019, pp. 1–6.
[40] M. Iqbal, J. Imtiaz, A. Mahmood, Bond graph modeling with linear quadratic integral control synthesis of a robotic digit in a human impaired hand for anthropomorphic coordination, Trans. Inst. Meas. Control 45 (3) (2023) 400–413, https://doi.org/10.1177/01423312221111643.
[41] G. Zames, Feedback and optimal sensitivity: model reference transformations, multiplicative seminorms, and approximate inverses, IEEE Trans. Autom. Control 26 (2) (1981) 301–320.
[42] S. Skogestad, I. Postlethwaite, Multivariable Feedback Control: Analysis and Design, John Wiley & Sons, 2005.
[43] A. Karimi, C. Kammer, A data-driven approach to robust control of multivariable systems by convex optimization, Automatica 85 (2017) 227–233.
[44] Q.M. Li, Y.P. Lv, A Fuzzy PID Control Method for the Grasping Force of an Underactuated Prosthetic Hand, Applied Mechanics and Materials, vol. 551, Trans Tech Publ, 2014, pp. 514–522.
[45] R. Raj, R. Ramakrishna, K.S. Sivanandan, A real time surface electromyography signal driven prosthetic hand model using PID controlled DC motor, Biomed. Eng. Lett. 6 (4) (2016) 276–286.
[46] D. Karnopp, D.L. Margolis, R.C. Rosenberg, System Dynamics, Wiley, New York, 1990.
[47] R.R. Rosenberg, D.C. Karnopp, Introduction to Physical System Dynamics, McGraw-Hill, Inc., 1983.
[48] L.A. Wojcik, Modeling of musculoskeletal structure and function using a modular bond graph approach, J. Franklin Inst. 340 (1) (2003) 63–76.
[49] A. Cole, J. Hauser, S. Sastry, Kinematics and control of multifingered hands with rolling contact, in: Proceedings, 1988 IEEE International Conference on Robotics and Automation, IEEE, 1988, pp. 228–233.
[50] S. Cobos, M. Ferre, M.S. Uran, J. Ortego, C. Pena, Efficient human hand kinematics for manipulation tasks, in: 2008 IEEE/RSJ International Conference on Intelligent Robots and Systems, IEEE, 2008, pp. 2246–2251.
[51] F. Chen Chen, A. Favetto, M. Mousavi, E. Ambrosio, S. Appendino, D. Manfredi, F. Pescarmona, G. Calafiore, B. Bona, Human hand: kinematics, statics, and dynamics, in: 41st International Conference on Environmental Systems, 2011, p. 5249.
[52] P. Slade, A. Akhtar, M. Nguyen, T. Bretl, Tact: design and performance of an open-source, affordable, myoelectric prosthetic hand, in: 2015 IEEE International Conference on Robotics and Automation, ICRA, IEEE, 2015, pp. 6451–6456.
[53] B. De Schutter, Minimal state-space realization in linear system theory: an overview, J. Comput. Appl. Math. 121 (1–2) (2000) 331–354.
[54] G.D. Forney, Minimal realizations of linear systems: the “shortest basis” approach, IEEE Trans. Inf. Theory 57 (2) (2011) 726–737.
[55] H. Rosenbrock, A. MacFarlane, State-space and multivariable theory, IEEE Trans. Syst. Man Cybern. 2 (1972) 295–296.
[56] J. Friedman, T. Flash, Trajectory of the index finger during grasping, Exp. Brain Res. 196 (4) (2009) 497–509.
[57] A. Gupta, G.S. Rash, N.N. Somia, M.P. Wachowiak, J. Jones, A. Desoky, The motion path of the digits, J. Hand Surg. 23 (6) (1998) 1038–1042.
[58] D.G. Kamper, E.G. Cruz, M.P. Siegel, Stereotypical fingertip trajectories during grasp, J. Neurophysiol. 90 (6) (2003) 3702–3710.
[59] J.C. Doyle, Structured uncertainty in control system design, in: 1985 24th IEEE Conference on Decision and Control, IEEE, 1985, pp. 260–265.
[60] E.L. Secco, A. Visioli, G. Magenes, Minimum jerk motion planning for a prosthetic finger, J. Robot. Syst. 21 (7) (2004) 361–368.
[61] W.G. Darling, K.J. Cole, Muscle activation patterns and kinetics of human index finger movements, J. Neurophysiol. 63 (5) (1990) 1098–1108.
[62] N.M. Kakoty, S.M. Hazarika, M.H. Koul, S.K. Saha, Model predictive control for finger joint trajectory of tu biomimetic hand, in: 2014 IEEE International Conference on Mechatronics and Automation, IEEE, 2014, pp. 1225–1230.
[63] I. Jo, Y. Park, J. Lee, J. Bae, A portable and spring-guided hand exoskeleton for exercising flexion/extension of the fingers, Mech. Mach. Theory 135 (2019) 176–191.
[64] J. Yang, H. Xie, J. Shi, A novel motion-coupling design for a jointless tendon-driven finger exoskeleton for rehabilitation, Mech. Mach. Theory 99 (2016) 83–102.
[65] J.Y. Loo, C.P. Tan, S.G. Nurzaman, H-infinity based extended Kalman filter for state estimation in highly non-linear soft robotic system, in: 2019 American Control Conference, ACC, IEEE, 2019, pp. 5154–5160.
[66] L. Zhao, H. Cheng, T. Wang, Sliding mode control for a two-joint coupling nonlinear system based on extended state observer, ISA Trans. 73 (2018) 130–140.
[67] H.F. Ali, A.M. Khan, H. Baek, B. Shin, Y. Kim, Modeling and control of a finger-like mechanism using bending shape memory alloys, Microsyst. Technol. 27 (6) (2021) 2481–2492.
[68] U.K. Alam, K. Shedd, M. Haghshenas-Jaryani, Trajectory control in discrete-time nonlinear coupling dynamics of a soft exo-digit and a human finger using input–output feedback linearization, Automation 4 (2) (2023) 164–190, https://doi.org/10.3390/automation4020011.